Journal of Computer-Aided Molecular Design **18:** 785–796, 2004.
DOI 10.1007/s10822-004-7878-1

Human topoisomerase I poisoning: docking protoberberines into a structure-based binding site model

Viktor Kettmann[a,*], Daniela Košťálová[b] & Hans-Dieter Höltje[c]
[a]*Department of Pharmaceutical Analysis and Nuclear Pharmacy, Faculty of Pharmacy, Comenius University, SK-83232 Bratislava, Slovakia;* [b]*Department of Pharmacognosy and Botany, Faculty of Pharmacy, Comenius University, SK-83232 Bratislava, Slovakia;* [c]*Department of Pharmaceutical Chemistry, Heinrich-Heine University, D-40225 Düsseldorf, Germany*

Received 7 May 2004; accepted in revised form 14 December 2004

Key words: anti-cancer drugs, human topoisomerase I poisoning, protoberberine alkaloids, structure-based molecular modeling

Summary

Using the X-ray crystal structure of the human topoisomerase I (top1) – DNA cleavable complex and the Sybyl software package, we have developed a general model for the ternary cleavable complex formed with four protoberberine alkaloids differing in the substitution on the terminal phenyl rings and covering a broad range of the top1-poisoning activities. This model has the drug intercalated with its planar chromophore between the −1 and +1 base pairs flanking the cleavage site, with the nonplanar portion pointing into the minor groove. The ternary complexes were geometry-optimized and relative interaction energies, computed by using the Tripos force field, were found to rank in correct order the biological potency of the compounds; in addition, the model is also consistent with the top1-poisoning inactivity of berberine, a major prototype of the protoberberine alkaloids. The model might serve as a rational basis for elaboration of the most active compound as a lead structure, in order to develop more potent top1 poisons as next generation anti-cancer drugs.

Introduction

Over the last decade, isoquinoline (protoberberine) alkaloids (Figure 1) have attracted considerable attention as they display a wide range of biochemical and pharmacological actions [1–3], the antineoplastic activity being one of the most important [4]; their cytotoxic activities have been demonstrated against numerous cancer cell lines (see, e.g. [5–7]). The overall biological profile of protoberberines [7] is very similar to camptothecin and its derivatives, some of which are currently in clinical use for the treatment of a variety of solid cancers [8]. Recently, protoberberines have also been shown to share a common mechanism of the cytotoxic action with the camptothecin family of drugs; the cytotoxic activities of these compounds are derived from DNA topoisomerase I (top1) poisoning, i.e. the ability to stabilize the ternary complex DNA – top1 – drug in its cleavable state [9, 10].

Normally, in the absence of drug, top1 plays a key role in relaxing supercoiled DNA for replication and transcription [11]. Top1 relaxes DNA by transiently beaking one strand of duplex DNA (in contrast to topoisomerase II which cleaves both strands of the duplex) through which the active site tyrosine (Tyr723, human top1) forms a phosphoester bond with the 3′-phosphate at a site of

*To whom correspondence should be addressed. E-mail: kettmann@fpharm.uniba.sk

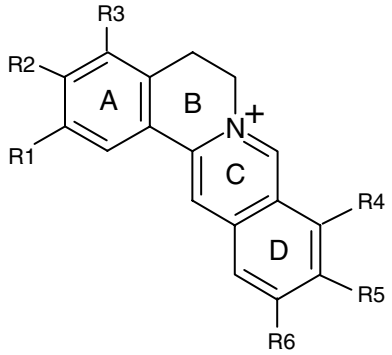

Figure 1. General chemical formula of protoberberines.

cleavage (−1 position) while a free 5'OH is formed at the other side (+1 position) (Figure 2) [12]; top1 subsequently religates the cleaved DNA and this is just the step in the catalytic cycle that is inhibited by the top1 poisons [13]. In the cell, drug-stabilized top1–DNA cleavage complexes generate cytotoxic double-strand DNA breaks after collision with replication forks [14, 15]. Thus, the top1 poisons are prominent anticancer drugs as the cancer cell damaged by fragmentation of the nuclear DNA typically respond by the cell cycle arrest in the G2/M phase which ultimately leads to apoptotical death of the cancer cell [4, 16, 17].

In view of their clinical importance, the camptothecin derivatives have been extensively studied by a number of techniques in order to develop novel drugs with improved therapeutic profile. Although extremely difficult, the crystal structure of their macromolecular target – the human top1 in a covalent (binary) complex with a 22-mer B-DNA – has also been determined at 2.1-Å resolution [18]. The structure showed that, due to two base-specific H-bond interactions, one between Lys532 and the O2 atom of −1 thymine (scissile strand) and the other between Arg364 and the N3 atom of −1 adenine (nonscissile strand), the top1

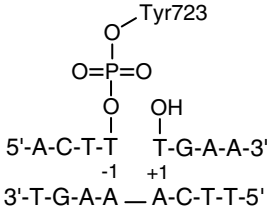

Figure 2. Schematic diagram of the cleavage site.

breaking sites have an A–T pair at position −1; in contrast, position +1 does not show any base-pair preference (in the absence of drug). Recently, three structure-based models of the interaction of the camptothecin derivatives with the covalent DNA–top1 complex have been proposed [18–20]; although the models are in many aspects contradictory, there is a consensus as well as experimental evidence [21, 22] that the drug intercalates between the cleavage site −1/+1 base pairs and favourably interacts with the enzyme as well.

In contrast to camptothecins, only a few reports appeared in the literature concerning the binding mode of protoberberines. In one of the most important studies [9] it was shown that (i) the planar (aromatic) system of rings C and D (Figure 1) is involved in an intercalative interaction with the duplex DNA whereas rings A and B protrude out of the helix interior into the minor groove where they interact with the minor-groove and/or top1 functionalities and (ii) all four protoberberines (**1–4**) depicted in Figure 3 unwind the B-DNA by approximately 11° due to the partial intercalative binding; this helix unwinding angle is in excellent agreement with the 10° value reported earlier by other inevestigators for the DNA binding of berberine, a structurally similar protoberberine to those studied here (Figure 3) [23, 24]. Recently, computer modeling techniques have also been employed to study the intercalative binding of some protoberberines with a $d(ApT)_2$ minihelix, but no correlation between the binding energy and the top1 poisoning activity was observed [9, 10], indicating that the interaction of the drug with top1 residues makes a significant contribution to the stability of the ternary drug – DNA – top1 cleavable complex. However, the amino acid residues of the enzyme could not be taken into account as the latter studies were conducted before the X-ray structure of the top1–DNA complex was available. Thus, in this paper, we were prompted to utilize not only the crystal structure of the top1-DNA cleavable complex but also the so far accumulated knowledge (outlined above) on both camptothecin and protoberberine families of drugs in order to derive structural models for the ternary drug–top1–DNA cleavable complexes (formed with selected protoberberine analogues) compatible with the known structure-activity relationships (SARs) and hence to establish a rational

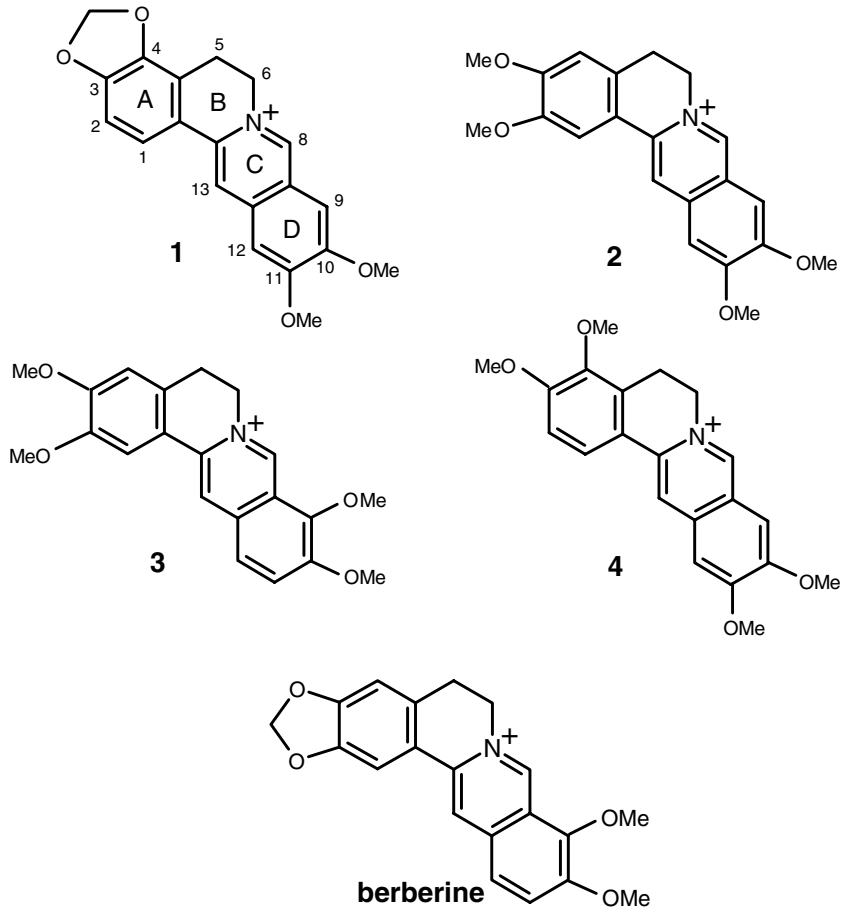

Figure 3. Chemical structures of the protoberberine analogues studied in this work (atomic numbering and ring lettering are indicated in the structure of (**1**) : 5,6-dihydro-3,4-methylenedioxy-10,11-dimethoxydibenzo[a,g]quinolizinium (**1**); 5,6-dihydro-2,3,10,11-tetramethoxydibenzo[a,g]-quinolizinium (**2**); 5,6-dihydro-2,3,9,10-tetramethoxydibenzo[a,g]quinolizinium (**3**, palmatine); 5,6-dihydro-3,4,10,11-tetramethoxydibenzo[a,g]quinolizinium (**4**); and 5,6-dihydro-2,3-methylene-dioxy-9,10-dimethoxydibenzo[a,g]quinolizinium (berberine).

basis for possible design of novel anticancer drugs.

Computational methods

All molecular modeling and energy calculations presented in this study were performed with a molecular modeling software package SYBYL [25] by using a two-step procedure.

Selection and conformational analysis of the compounds

In the first step, a ligand database containing compounds **1–4** and berberine (Figure 3) was prepared. The rationale for the selection of the compounds **1–4** for this study was the following: (i) the top1-poisoning activity data came from the same source [9] and were obtained by using the same experimental protocol and standard procedure [26], i.e. by measuring the relative extents to which they stimulate the top1-mediated DNA cleavage; (ii) the activity of the compounds varies in a broad range, spanning several orders of magnitude and can be ranked in the following order: **1** > **2** > > **3** ≥ **4**; the most active compound **1** is only 10-fold less potent stimulator of top1-induced DNA cleavage than camptothecin (used in clinical practice) and roughly 10-fold more potent compared to compound **2**; the difference in potency between compounds **2** and **3** is

at least 100-fold so that while **3** shows only marginal but still significant potency, the compound **4** is totally inactive (at 10 μM); and (iii) in contrast to the top1 poisoning activity, the structure and hence the hydrophobic effect (proportional to the change in solvent-accessible surface area due to binding) for the four compounds varies only minimally so that solvent effects might be neglected in the calculations of interaction (binding) energy [27].

To explore the conformational mobility of the protoberberine skeleton, molecular dynamics (MD) simulations were performed by using the standard Tripos force field. Initial structures were taken from the crystal structure of berberine chloride [28] and the substitution modified by using the 'Sketch Molecule' in Sybyl. MD runs, performed arbitrarily on palmatine, were simulated at 300 K; while the molecule was maintained at this temperature for 100 ps, snapshots of its conformation were taken at 2-ps intervals and each of the 50 conformations obtained were full-energy minimized by the Sybyl/Maximin2 routine; the minimized conformations were finally analysed by the Family option of the Sybyl/Table routine. As to the substituents, the two ortho methoxy groups (in the 2,3- or 10,11-positions) were assumed to adopt the coplanar conformations due to conjugation energy of the lone-pair electrons on the O atoms with the adjacent aromatic system and sterically unhindered positions of the terminal methyl groups; we verified the coplanarity of these methoxy groups by analysing the compounds containing the 1,2-dimethoxybenzene moiety present in the Cambridge Structural Database (CSD) [29]. A different situation is expected for a sterically hindered rotation of the methoxy group in the 9-position of the 9,10-dimethoxy derivatives (palmatine and berberine). Therefore, the conformational energy curve for rotation of the 9-OCH_3 group around the C–O bond in palmatine was calculated by using the grid search routine with an angle increment of 10° and with full energy minimization except for the dihedral angle used as driving angle; the same energy profile was also computed by semiempirical AM1 method using the MOPAC package implemented in Sybyl; the starting points for the AM1 studies were taken from the atomic coordinates of the corresponding conformers obtained in the preceding molecular mechanics calculations.

Construction of the ternary complexes

The docking of the compounds into the active site of the top1–DNA covalent complex in order to create the ternary drug–top1–DNA complexes consisted of three steps: (1) preparation of the top1–DNA binary complex; (2) construction of a DNA (intercalation) cavity; and (3) docking of each compound into the cavity.

To prepare the top1–DNA complex, the coordinate file of the published X-ray crystal structure of the top1–DNA covalent complex (PDB code: 1a31) [18] was uploaded into the computer. The following modifications were made to this structure: (i) the iodouracils were converted to thymines; (ii) the crystallographic water molecules, except for the long-life [30] bridging water doubly hydrogen bonded to protonated Arg488 and ionized Asp533, were removed; (iii) hydrogen atoms were added to both the DNA and the enzyme; and (iv) the entire complex was energy minimized using the Tripos force field to the conjugate gradient of 1 kcal/(mol Å).

Next, the intercalation site and the downstream portion of the modified DNA was created by using the X-ray crystal structure of an intercalative complex of 9-amino-N-[2-(4-morholinyl)ethyl]-4-acridinecarbox-amide (DACA) with the B-DNA duplex $d(CGTACG)_2$ (PDB entry code: 1kci) [31] since DACA unwinds the DNA to the same extent (~10°) as does the protoberberine molecule and the interplanar separation between the two base pairs (~6.8 Å) corresponds to the mean value observed in a variety of ligand–DNA complexes as revealed by a search of the PDB file [32]. In short, the following procedure was adopted: (1) DACA, intercalated between the last two base pairs at the 3′ end of the oligonucleotide was removed; (2) as the asymmetric unit of the structure contains only one DNA strand (5′-CGTACG-3′), it was used to construct the downstream part of the nonscissile strand of the top1–DNA crystal structure: the G nucleotide at the 3′ end was mutated to adenine and aligned with the −1 adenine of the top1–DNA complex (the −1 thymine to which top1 is covalently bonded via Tyr723 was left intact); (3) the downstream portion of the scissile strand was built within Sybyl as the complement to the CATGC sequence; (4) finally, to simplify the model, the DNA substrate in the new top1–DNA complex (containing the

intercalation cavity) was cut at both sides to the octamer. These modifications resulted in the DNA sequence shown below:

$$\begin{array}{l} \quad\quad -1\ \ +1 \\ 5'\text{-A-C-T-T}\hat{}\text{G-T-A-C-}3' \\ 3'\text{-T-G-A-A–C-A-T-G-}5' \end{array}$$

where a caret between the central T and G bases indicates the cleavage site. Although the +1 base pair was initially built as the C–G pair, the remaining three combinations (G–C, A–T, and T–A) were also generated. To remove possible steric clashes of the modified DNA with the enzyme and, at the same time, to obtain the energy of the unadducted binary top1–DNA complex, a 12Å sphere of the complex about the intercalation site was energy minimized by using the Tripos force field until the rms value of the conjugate gradient fell below 0.1 kcal/(mol Å).

The docking was conducted in two stages. In the first stage, only the intercalative binding was taken into account and the Dock module of Sybyl was used for this purpose. Initially, the chromophore (rings C and D) of the compound was placed halfway between the −1 and +1 base pairs (i.e. the penalty for penetrating into the enzyme was set to zero) in such a way that the nonplanar portion (rings A and B) lay in the minor groove. Two orientations of the compound, A and B, related by a 180° rotation around the longitudinal axis of the molecule and differing in the position of the quaternary nitrogen right and left, respectively, when looking towards the minor groove, were considered as starting configurations. Then, small translations and rotations around the x, y, and z axes was applied to the molecule, in order to find its global energy minimum location in the intercalation site with respect to the sum of the van der Waals (E_{vdW}) and electrostatic (E_{el}) energy contributions:

$$E_{\text{intercalation}} = E_{vdW} + E_{el} \quad (1)$$

A 'rigid docking procedure' was adopted, i.e. the two interacting molecules were considered as rigid bodies. The energy was calculated in a rectangular box defined by the −1 and +1 base pairs. Finally, the manual docking procedure was followed by an automatic energy minimization using the minimize_dock command of Sybyl to give the final energy value $E_{\text{intercalation}}$ (Equation 1) corresponding to the optimal location of the compound in the intercalation site.

In the second stage, full-energy minimization of the ternary complexes were performed by adopting the same procedure as described above for the unadducted complex, i.e. by using Tripos force field (in which besides the two energy terms given in Equation 1 the possibility of hydrogen bonding was also taken into account) and allowing all atoms in a 12 Å sphere about the intercalation site to move freely [convergence criterion < 0.1 kcal/(mol Å)]. Throughout the calculations, the partial atomic charges were obtained by using Kollman All-atom method for the DNA and protein and Gasteiger-Hückel method for the ligands. Solvent effects were not considered in the calculations either explicitly by the inclusion of water molecules or implicitly by incorporation of dielectric effects; the dielectric constant was set to unity.

Having obtained the energy of each system, the interaction energy was estimated as follows:

$$E_{\text{interaction}} = E_{\text{complex}} - (E_{\text{compound}} + E_{\text{site}}) \quad (2)$$

where E_{compound} and E_{site} are the energies of the free compound and binding site, respectively. After the total energy minimization, a single-point intercalation energy calculation (i.e. without geometry optimization), was performed by using the Dock module and the same box size as used before the total energy minimization, in order to dissect the interaction energy (Equation 2) into two energy components corresponding to the interaction of the compound with the DNA and the enzyme.

Results and discussion

In this study, we examined structural and energetic features of the ternary complexes constructed by docking of four selected protoberberine alkaloids with known SARs into the binding site of the binary top1–DNA complex taken from the known X-ray structure of the covalent intermediate.

First, we performed detailed conformational analysis of the compounds studied here. MD runs have shown that the conformation of the protoberberine skeleton found in the crystal structure of berberine chloride [28] is stable under the MD simulations at ambient temperature: all 50 instantaneous conformations taken from the sampling procedure belonged to the same family characterized by approximately C6-envelope conformation

for the puckered (B) ring and differed from each other in the N–C13a–C13b–C4a torsion angle (α) which defines the tilting of the A ring with respect to the plane of the C-D chromophore; α varied in the range 16–27° and the subsequent full-geometry optimization relaxed to the same energy minimum $\alpha \approx 25°$. Somewhat smaller range of values for α (12–20°) has been found experimentally in compounds containing the protoberberine substructure as revealed by a search of CSD [29] ($n = 18$). As to the substitution pattern, while the 2,3- and 10,11-dimethoxy groups were kept in the most stable coplanar orientations, the full-energy profile for rotation of the 9-methoxy group in palmatine (compound **3**) and berberine was calculated by the molecular mechanics and the semiempirical AM1 methods, and the results are shown in Figure 4. As can be seen from the figure, both methods give $\varphi = 0°$ for the most stable conformation but the course of the curves is different. Interestingly, the φ values for such a methoxy group found in the X-ray structures of the protoberberine derivatives range from 10 to 65° ($n = 11$) implying that the Tripos force field fits better the experimental data as compared to the AM1 method.

Next, we were interested in calculating not only the total interaction energy of the ternary ligand–DNA–top1 complexes but also the DNA binding energy of the C–D chromophore before and after the full-energy minimization as well as sequence selectivity of the protoberberines. As noted above, the enzyme alone, in contrast to the −1 position, does not induce any base preference for the +1 position of the DNA. Therefore, we analysed the sequence specificity profile of the protoberberines

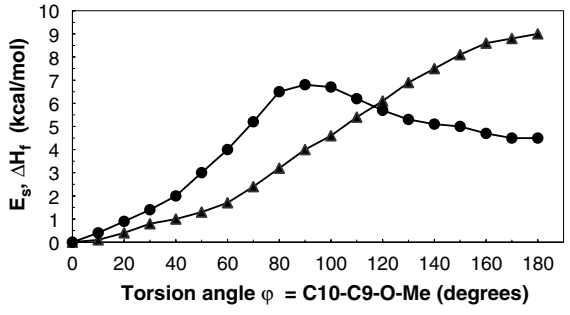

Figure 4. Energy profile for rotation of the 9-methoxy group around the C–O bond in palmatine as calculated by the Tripos force field (E_s – full triangles) and the AM1 method (ΔH_f – full circles).

by docking the most active compound **1** into the intercalation cavity possessing all four possible sequences in this (+1) position. However, the C–G and G–C sequences failed to yield stable structures during the initial stage of the docking procedure. In contrast, both orientations (A and B) of the compound in the intercalation site with either A–T of T–A base pairs in the +1 position gave stable docked structures. However, the intercalation energies of the four structures differed markedly. Specifically, intercalative mode A with +1 scissile strand thymine yielded the structure with the lowest energy and hence we selected this binding mode for further investigation. This result is in line with experimental evidence that the binding of the protoberberine alkaloids to contiguous A–T seqences is much favoured over binding to G–C or mixed sequences [6, 33].

A portion of the lowest energy structure described above for the ternary compound **1**–DNA–top1 cleavable complex is shown in Figure 5. In accordance with expectation, the C–D chromophore of **1** docks in the DNA intercalation cavity perpendicular to the main axis of the DNA, parallel to the −1/+1 bases, with the nonplanar (A–B) portion of the molecule projecting outward from the minor groove. Note that the two oxygen atoms of the D-ring 10,11-dimethoxy substituent lie within the intercalation site while the methyl groups protrude out towards the major groove where they interact with the atoms exposed to the major groove: the methyl of the 10-methoxy moiety is in favourable van der Waals interaction with the 5-methyl groups of both −1 and +1 thymines and the 11-methoxy methyl group is in close contact with the nonpolar atoms (C5, C6 of the −1/+1 adenine bases) lining the floor of the major groove. On the other side of the molecule, a number of polar and nonpolar interactions with the amino acid residues of top1 can be identified. Specifically, the O3 atom of the 3,4-methylenedioxy functionality makes a H-bond with Arg364 (O...N 2.8 Å) while retaining the base-specific H-bond with the −1 adenine (Figure 5); thus, Arg364 acts as a bridge between the −1 adenine and the drug molecule. Similarly, the O4 oxygen of the drug is within H-bonding distance of the water molecule (O...O 2.9 Å) which forms a bridge between Arg488 and Asp533. In the orientation of the ligand as shown in Figure 5, the hydrophobic (side chain) portion of Lys532, which is H-bonded

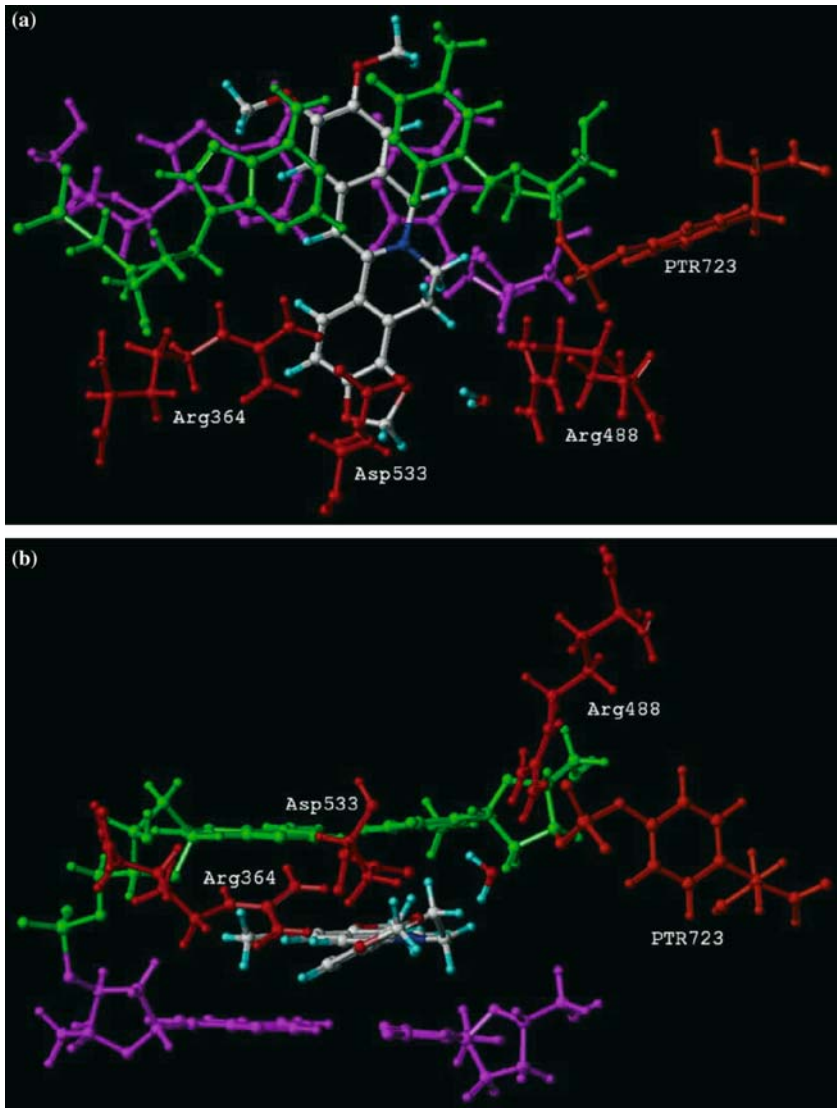

Figure 5. A portion of the refined structural model for the ternary ligand **1**–DNA–top1 cleavable complex. The colour coding scheme for the DNA nucleotides is as follows: the −1 adenine–thymine base pair, green; the +1 adenine–thymine base pair, violet. The top1 amino acid residues are depicted in red while the protoberberine and solvent water molecules are coloured by atom type (carbon, white; oxygen, red; nitrogen, blue; hydrogen, cyan). (a) A view looking down the helical axis. (b) A view looking from the minor groove and perpendicular to the helical axis.

to the −1 thymine, runs parallel with the B-ring and a part of the A-ring at the van der Waals separation (not shown in Figure 5 for clarity). Finally, the methylene group of the methylenedioxy moiety is in van der Waals contact with Ile535 (not shown). It is remarkable that compound **1** is able to achieve this pattern of H-bond and van der Waals interactions without any movement of either amino acid residues or the drug molecule from its optimal DNA binding position (Table 1; compare 'optimal' and 'minimized' drug–DNA interaction energies).

Close expection of Figure 5 also provides an explanation for the experimentally observed A–T base selectivity of the protoberberines; the additional NH_2 group at the 2-position of the +1 adenine (to convert it into the guanine) would create a steric clash of this amino group with the A-ring (*viz*. C1–H moiety) due to the tilting of this ring relative to the plane of the C–D chromophore;

Table 1. Ligand – DNA/top1 binding site interaction energies.

Ligand	Ligand – DNA			Ligand – top1		Total energy[a]
	Optimal[b]	Minimized[b]		E_{el}[c]	E_{vdW}[c]	(kcal/mol)
		E_{el}[c]	E_{vdW}[c]			
1	−45.5	−10.5	−34.4	−16.6	−7.2	−68.7
2	−45.5	−9.2	−33.8	−11.4	−7.5	−61.9
3[d]	−38.4	−3.5	−28.7	−10.1	−4.5	−46.8
4	−45.5	−3.9	−29.5	−6.9	−3.3	−43.6
berberine	−29.9	2.6	−24.4	−16.1	−7.1	−45.0

[a]The total interaction energies were broken into two components corresponding to the interaction of each ligand with the DNA and protein (top1).
[b]Optimal and minimized ligand – DNA binding energies correspond, respectively, to the interaction energies between the ligand and the DNA intercalation cavity before and after the total-energy minimization (see text).
[c]Electrostatic (E_{el}) and van der Waals (E_{vdW}) contributions to the ligand – DNA and ligand – enzyme interaction energies.
[d]Palmatine.

in order to relieve this negative steric interaction, the molecule would be forced to be repositioned from its optimal orientation with concomitant loss of some important interactions.

The model of the ternary complex with compound **2** (not shown) reveals very similar structural features compared to that of compound **1** as far as the position in the DNA binding cavity and energies are concerned (Table 1). However, as the structural difference between compounds **1** and **2** concerns the chemical substitution on the A-ring (Figure 4), which lies in the minor groove, the energy term arising from the interaction with the enzyme is different. First, the water-mediated H-bond interaction with Arg488 and Asp533 is lost but, as the O3–CH_2-moiety in **1** is spatially equivalent to the O3–CH_3 methoxy group in **2**, the H-bonding and the van der Waals interactions of the 3-methoxy group with Arg364 and Ile535, respectively, are maintained. The loss of one H-bond in **2** (relative to **1**) is reflected in a ca. 5-kcal/mol lowering of the drug–top1 interaction energy (Table 1); in addition, as shown in Table 1, there is also some reduction of the DNA binding energy most likely due to slight movement of the drug molecule in order to optimize the H-bond geometry with Arg364.

In contrast to compounds **1** and **2**, compd. **3** (palmatine) differs from the former in the intercalative portion of the molecule (D-ring) and the conformational flexibility of the 9-methoxy group. Therefore, besides considering the intercalative modes A and B, the total interaction energy of the ternary complex with palmatine was calculated as a function of the torsion angle φ (C10–C9–O–Me) which was allowed to vary from −60 to +60° in 10°-steps. The calculations have shown that the most stable ternary complex adopts the A binding mode and coplanarity of the 9-methoxy group with the aromatic system ($\varphi = 0$). Docking of **3** into the DNA intercalation site yielded the structure (Figure 6) which is different from that of **1** (or **2**) (compare Figures 5 and 6), with the intercalation energy being lower in magnitude (Table 1). Moreover, another destabilizing factor became obvious during the second stage of the docking procedure, *viz*. negative steric contact of the 2-OCH_3 group with Arg364 which was removed during the total-energy minimization by unfavourable tilting of the molecule out of the plane of the bases accompanied by further decrease of the DNA-binding energy (Table 1). The net result is poor docking of palmatine in the DNA–top1 binding site which accounts for the large decrease in the top1-poisoning activity of **3** relative to **1** and **2**.

Finally, the structure and energetics of the ternary complex with the inactive compound **4** can best be visualized by referring to Figure 5. Due to our docking strategy, the lowest energy DNA-docked structure obtained from the first stage of the docking procedure (i.e. ignoring the top1 residues) is identical to that shown in Figure 5. However, while the position of the lone-pair electrons of both A-ring oxygens in **1** was optimal for accepting H-bonds from Arg364 and the solvent water, in **4** the lone-pairs are replaced by bulky methyl groups so that they almost collide with the

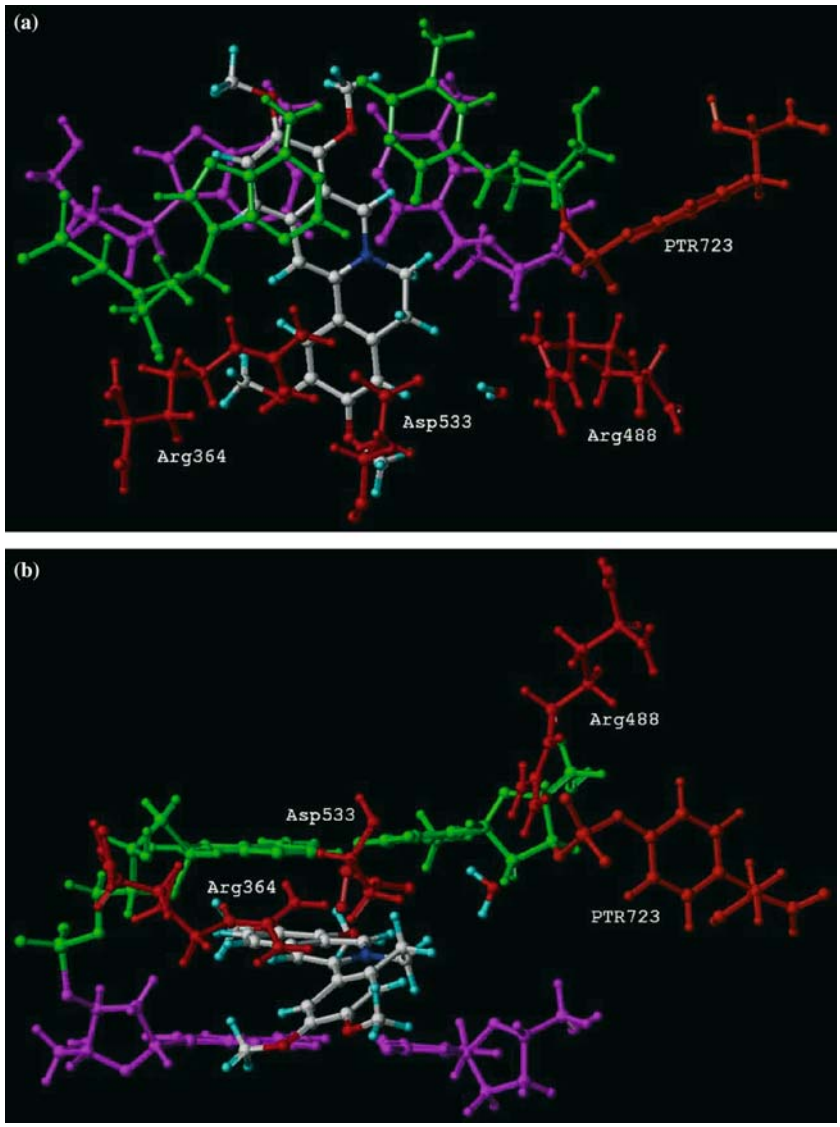

Figure 6. A portion of the refined structural model for the ternary ligand **3**–DNA–top1 cleavable complex. The colour coding scheme is the same as in Figure 5. (a) A view looking down the helical axis. (b) A view looking from the minor groove and perpendicular to the helical axis.

Arg364 side chain and the water molecule. The subsequent full-geometry optimization has shown that the steric collision is again removed by a tilt of the molecule from the plane of the bases but this rearrangement is even more drastic in **4** (not shown) as compared to **3** (Table 1).

As shown in Table 1, for the four compounds studied here, there is a clear-cut correlation between the relative interaction energy and the rank order of the top1-poisoning activity (see above). The existence of this correlation has some important implications: (1) For a congeneric series of compounds force-field-derived interaction energies yield meaningfull results as mentioned earlier [34]; thus, ignoring change in entropy and desolvation energy of the compounds may be a good approximation to the binding free energy (binding affinity) if these terms are comparable for all the compounds studied. (2) The molecular mechanism of the top1 poisoning activity (DNA fragmentation) of the protoberberine alkaloids lies in preventing religation of the cleaved strand during the

catalytic cycle, which in turn is a result of intercalation of the drug between the base pairs of the cleavage site; the intercalation effectively displaces the downstream DNA and hence keeps the terminal 5′OH out of the attacking distance from the phosphate group of the 3′-phosphotyrosine inermediate.

In the next part of the study we used the model of the DNA–top1 binding site to account for the biological profile of berberine, a major representative of the protoberberine alkaloids, which has been found to be predominantly distributed in several genera of the families Ranunculaceae and Berberidaceae (e.g. Berberis, Mahonia, Coptis). Various groups [5–7, 17, 35–38] have demonstrated modest *in vitro* anticancer potency of berberine against numerous (including human) cancer cell lines (the 50% inhibitory concentration varies in the range of 1–10 μg/ml) and its ability to induce apoptosis, a hallmark of both top1- and top2-poisons. However, it was reported [36] that berberine is able to stimulate enzyme-mediated DNA cleavage only with top2 but not with top1 enzyme. To test the ability of our model to explain the lack of top1-poisoning activity of berberine, we applied our docking methodology to the latter compound. The results have shown that although the intercalative mode A is lower in energy (as in palmatine), the total interaction energy was found to be lower as compared to mode B, obviously due to unfavourable positioning of the non-intercalative portion of the molecule in the minor groove. On the other hand, the mode B, though higher in energy (Table 1), places the A-ring 2,3-methylenedioxy moiety in the optimal position for interaction with the top1 residues (Figure 7; Table 1). In this respect berberine resembles the most active compound **1** (compare Figures 5a and 7a) but, in contrast to **1**, berberine achieves this favourable interaction with top1 at the expense of the DNA-binding energy and hence the total interaction energy of berberine is only slightly higher than that of the inactive compound **4** (Table 1).

As mentioned in Introduction, the discovery of the top1-poisoning activity of the protoberberines has naturally generated interest in their potential clinical utility as anti-cancer agents [4–7, 9, 10]. Comparisons of the biological properties of the protoberberines with those of the camptothecins, which are the only top1 inhibitors in clinical use, has revealed a number of differences that might be advantageous for the protoberberines. First, in contrast to the camptothecins, which are inactivated by lactone hydrolysis at physiological pH [19], the protoberberines are chemically stable. Second, the protoberberines induce a unique pattern of DNA cleavage sites relative to camptothecins [6, 33, 39], indicating that they may target the human genome differently and hence potentially exhibit a different spectrum of anticancer activity from the camptothecins [40, 41]. However, the most severe factor which markedly limit the clinical use of the camptothecins is their toxicity profile; these compounds present a narrow therapeutic index, with a small difference between the dose required for an antitumour effect and that responsible for unacceptable toxicity; in addition, toxicity is observed earlier than the therapeutic effect [42]. Especially a dose-related and irreversible cardiotoxicity of the camptothecins is often life-threatening [43]. These unwanted side effects are lacking for the protoberberine derivatives even at high dosages so that they have a chance to replace the camptothecins in future. The drawback of the protoberberines is in turn their moderate potency, both in mediating the top1-poisoning and the cytotoxic activities, which is 1–2 orders of magnitude lower relative to camptothecins. Thus, to enhance the binding energy would be desirable in order to increase the cytotoxic potency and hence the significance of the protoberberines as potential anti-cancer drugs.

Concluding remarks

In this study, we have used the X-ray crystal structure of the binary top1–DNA cleavable complex, in combination with the current knowledge on the structural and biological properties of the camptothecin and protoberberine families of drugs, to construct structure-based models for ternary complexes formed between a series of protoberberines and the active site of the binary complex. The validity of the models was verified by a correlation between the calculated stability of the complexes and the experimentally determined top1-poisoning activity. Thus, the ternary model formed with the most active (lead) compound **1** could serve as a guide in searching for additional interactive site(s) in the enzyme in order to enhance the cytotoxic potency of the protoberberine

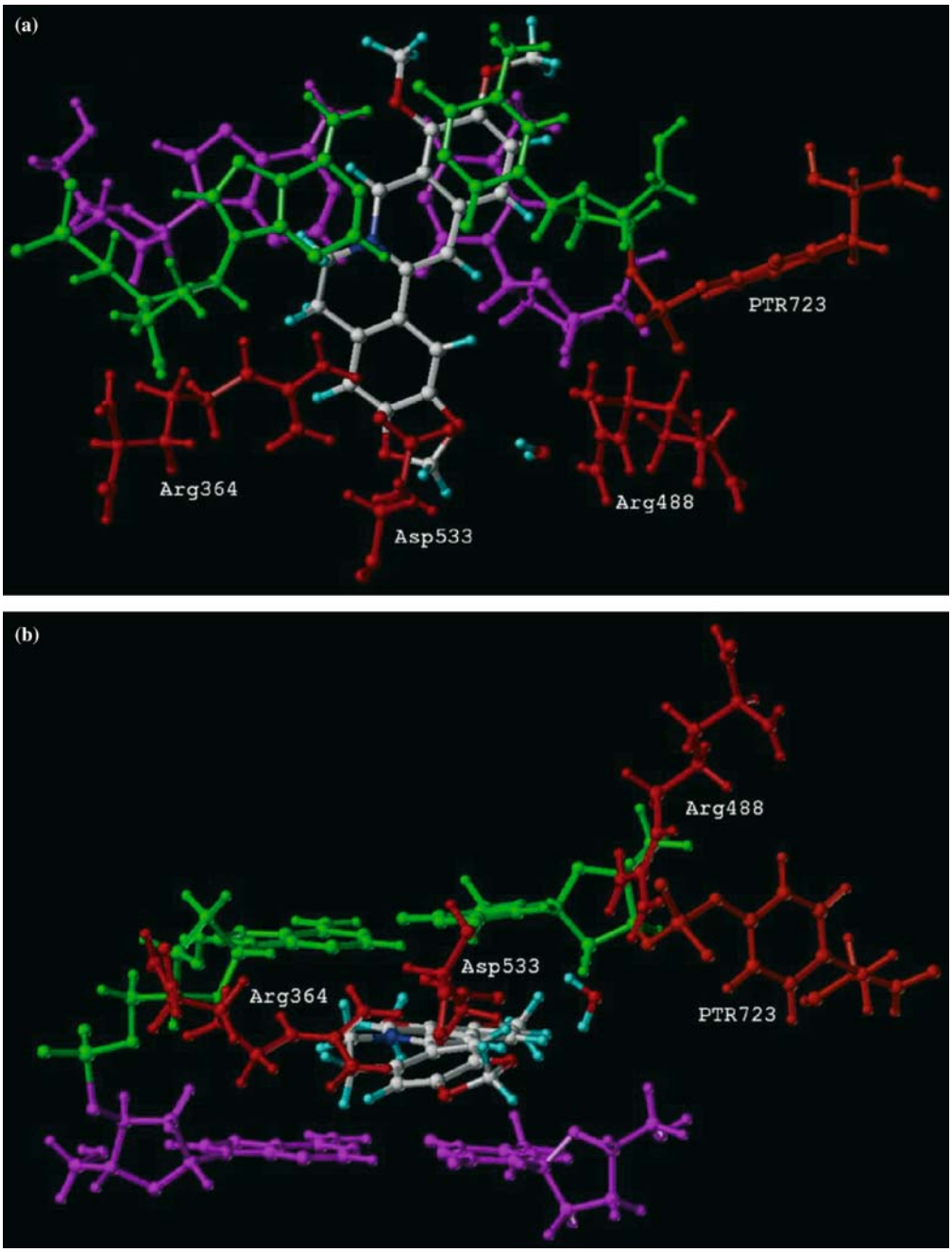

Figure 7. A portion of the refined structural model for the ternary berberine–DNA–top1 cleavable complex. The colour coding scheme is the same as in Figure 5 (see on-line version). (a) A view looking down the helical axis. (b) A view looking from the minor groove and perpendicular to the helical axis.

molecule. The results obtained here indicate that while the 3,4-methylenedioxy substitution on the A-ring in **1** seems to be optimal for the interaction of the molecule with the pattern of the top1 amino acid residues circling the DNA minor groove, the substituents attached to the D-ring could be elaborated to come into interaction with a number of polar and nonpolar enzyme residues present in the major groove. Such work is going to start in our laboratory and will be published later.

Acknowledgements

This research was supported by Grant Agency of the Slovak Republic, Grant Nos. 1/1167/04, 1/1185/04, and 1/1196/04.

References

1. Okunade, A.L., Hufford, C.D., Richardson, M.D., Petterson, J.R. and Clark A.M., J. Pharm. Sci., 83 (1994) 404.
2. Sarma, B.K., Pandey, V.B., Mishra, G.D. and Singh, U.P., Folia Microbiol., 44 (1999) 164.
3. Èeròáková M., Košťálová, D., Kettmann, V., Plodová M., Tóth, J. and Døímal J.BMC Complement. Alternative Med., 2 (2002) 1.
4. Kuo, C.L., Chou, C.C. and Yung B.Y.-M., Cancer Lett., 93 (1995) 193.
5. Orfila, L., Rodriguez, M., Colman, T., Hasegawa, M., Merentes, M. and Arvelo, F., J. Ethnopharmacol., 71 (2000) 449.
6. Iwasa, K., Moriyasu, M., Yamori, T., Turuo, T., Lee, D.U. and Wiegrebe, W., J. Nat. Prod. 64 (2001) 896.
7. Kettmann, V., Košťálová, D., Jantová, S., Èeròáková, M. and Døímal, J., Pharmazie, 59 (2004) 548.
8. Pantazis, P., Giovanella, B. and Rotenberg, M.L., The Camptothecins: From Discovery to the Patient. New York Academy of Sciences, New York, 1996.
9. Li, T.K., Bathory, E., LaVoie, E.J., Srinivasan, A.R., Olson, W.K., Sauers, L.L., Liu, L.F. and Pilch, D.S., Biochemistry, 39 (2000) 7107.
10. Pilch, D.S., Yu, C., Makhey, D., LaVoie, E.J., Srinivasan, A.R., Olson, W.K., Sauers, R.R., Breslauer, K.J., Geacintov, N.E. and Liu, L.F., Biochemistry, 36 (1997) 12542.
11. Champoux, J., In Wang, J.C. and Cozarelli, N.R. (Eds.), DNA Topology and its Biological Effects, Cold Spring Harbor Laboratory Press, Cold Spring Harbor, NY, 1990, pp. 217–242.
12. Wang, J.C., Ann. Rev. Biochem., 65 (1996) 635.
13. Hsiang, Y.H., Hertzberg, R., Hecht, S. and Liu, L.F., J. Biol. Chem., 260 (1985) 14873.
14. Ryan, A.J., Squires, S., Strutt, H.L. and Johnson, R.T., Nucleic Acids Res., 19 (1991) 3295.
15. Snapka, R.M. and Permana, P.A., Bioessays, 15 (1993) 121.
16. Yang, I.W., Chou, C.C. and Yung, B.I.M., Naunyn-Schiedeberg's Arch. Pharmacol., 354 (1996) 102.
17. Jantová, S., Čipák, L'., Čeròáková, M. and Košťálová, D., J. Pharm. Pharmacol., 55 (2003).
18. Redinbo, M.R., Stewart, L., Kuhn, P., Champoux, J.J. and Hol, W.G.J., Science, 279 (1998) 1504.
19. Laco, G.S., Collins, J.R., Luke, B.T., Kroth, H., Sayer, J.M., Jerina, D.M. and Pommier, Y., Biochemistry, 41 (2002) 1428.
20. Kerrigan, J.E. and Pilch, D.S., Biochemistry, 40 (2001) 9792.
21. Pommier, Y., Laco, G.S., Kohlhagen, G., Sayer, J.M., Kroth, H. and Jerina, D.M., Proc. Natl. Acad. Sci. USA, 97 (2000) 10739.
22. Staker, B.L., Hjerrild, K., Feese, M.D., Behnke, C.A. and Stewart, L., Proc. Natl. Acad. Sci. USA, 99 (2002) 15387.
23. Davidson, M.W., Lopp, I., Alexander, S. and Wilson, W.D., Nucleic Acids Res., 4 (1977) 2697.
24. Jones, R.L., Lanier, A.C., Kiel, R.A. and Wilson, W.D., Nucleic Acids Res., 8 (1980) 1613.
25. SYBYL: Tripos Associates Inc., St. Louis, MO; version 6.7.
26. Hsiang, Y.-H., Hertzberg, R., Hecht, S. and Liu, L.F., J Biol. Chem., 260 (1985) 14873.
27. Wang, R., Lai, L. and Wang, S., J. Comput.-Aided Mol. Des., 16 (2002) 11.
28. Kariuki, B.M. and Jones, W., Acta Crystallogr., Sect. C, 51 (1995) 1234.
29. Allen, F.H., Kennard, O. and Taylor, R., Acc. Chem. Res., 16 (1983) 146.
30. Chillemi, G., Castrignano, T. and Desideri, A., Biophys. J., 81 (2001) 490.
31. Adams, A., Guss, J.M., Denny, W.A. and Wakelin, L.P.G., Nucleic Acids Res., 30 (2002) 719.
32. Berman, H.M., Westbrook, J., Feng, Z., Gilliland, G., Bhat, T.N., Weissig, H., Shindyalov, I.N. and Bourne, P.E., Nucleic Acids Res., 28 (2000) 235, http://www.rcsb.org/pdb/.
33. Pilch, D.S., Yu, C., Makhey, D., LaVoie, E.J., Srinivasan, A.R., Olson, W.K., Sauers, R.R., Breslauer, K.J., Geracintov, N.E. and Liu, L.F., Biochemistry, 36 (1997) 12542.
34. Wang, R., Lai, L. and Wang, S., J. Comput.-Aided Mol. Des., 16 (2002) 11.
35. Anis, K.V., Kuttan, G. and Kuttan, R., Pharm. Pharmacol. Commun., 5 (1999) 697.
36. Kobayashi, Y., Yamashita, Y., Fujii, N., Takaboshi, K., Kawakami, T., Kawamura, M., Mizukami, T. and Nakano, H., Planta Med., 61 (1995) 414.
37. Li, T.-K., Bathory, E., LaVoie, E.J., Srinivasan, A.R., Olson, W.K., Sauers, R.R., Liu, L.F. and Pilch, D.S., Biochemistry, 39 (2000) 7107.
38. Krishnan, P. and Bastow, K.F., Anti-Cancer Drug Des., 15 (2000) 255.
39. Fan, Y., Weinstein, J.N., Kohn, K.W., Shi, L.M. and Pommier, Y., J. Med. Chem., 41 (1998) 2216.
40. Palumbo, A., Gatto, B., Moro, S., Sissi, C. and Zagotto, G., Biochim. Biophys. Acta, 1587 (2002) 145.
41. Sanders, M.M., Liu, A.A., Li, T.-K., Wu, H.-Y., Desai, S.D., Mao, Y., Rubin, E.H., LaVoie, E.J., Makhey, D. and Liu, L.F., Biochem. Pharmacol., 56 (1998) 1157.
42. Chatelut, E., Delord, J.P. and Canal, P., Invest. New Drugs, 21 (2003) 141.
43. Pantazis, P. and Giovanella, B., In Rotenberg, M.L. (Ed.), The Camptothecins: From Discovery to the Patient, New York Academy of Sciences, New York, 1996, pp. 1–328.